

1 **Evaluation of additional physiographical variables characterising drainage network**
2 **systems in regional frequency analysis, a Quebec watersheds case-study**

3

4 A. Msilini^{1, *}, T.B.M.J. Ouarda¹ and P. Masselot²

5 ¹*Canada Research Chair in Statistical Hydro-Climatology, INRS-ETE, 490 de la Couronne,*
6 *Québec, QC, G1K 9A9, Canada.*

7 ²*London School of Hygiene & Tropical Medicine (LSHTM), 15-17 Tavistock Pl, London, WC1H*
8 *9SH, United Kingdom.*

9 * Corresponding author: Amina Msilini (amina.msilini.m@gmail.com)

10 **Acknowledgments and Data**

11 Financial support for the present study was graciously provided by the Natural Sciences
12 and Engineering Research Council of Canada (NSERC), the Canada Research chairs
13 program (CRC) and the University Mission of Tunisia in Montreal (MUTAN). The
14 authors would like to thank Christian Charron for his valuable help and input. The
15 authors are grateful to Natural Resources Canada ([https://www.nrcan.gc.ca/earth-](https://www.nrcan.gc.ca/earth-sciences/geography/topographic-information/download-directory-documentation/17215)
16 [sciences/geography/topographic-information/download-directory-documentation/17215](https://www.nrcan.gc.ca/earth-sciences/geography/topographic-information/download-directory-documentation/17215))
17 and the USGS (<https://earthexplorer.usgs.gov/>) services for the employed DEM and
18 NHN data. The authors would like also to thank the Ministry of Sustainable
19 Development, Environment, and Fight Against Climate Change (MDDELCC) services
20 for the used dataset (STA). The authors are grateful to the Editor-in-Chief, Dr. George
21 Christakos, and to three anonymous reviewers for their comments which helped improve
22 the quality of the manuscript.

23 **Conflicts of Interest:** The author declares no conflict of interest.

24

August, 2021

25 **Abstract**

26 Regional Frequency Analysis (RFA) relies on a wide range of physiographical and
27 meteorological variables to estimate hydrological quantiles at ungauged sites. However,
28 additional catchment characteristics related to its drainage network are not yet fully
29 understood and integrated in RFA procedures. The aim of the present paper is to propose
30 the integration of several physiographical variables characterizing the drainage network
31 systems in RFA, and to evaluate their added value in predicting quantiles at ungauged
32 sites. The proposed extended dataset (EXTD) includes several variables characterising
33 drainage network characteristics. To evaluate the new variables, a number of commonly
34 used RFA approaches are applied to the extended data representing 151 stations in
35 Quebec (Canada) and compared to a standard dataset (STA) that excludes the new
36 variables. The considered RFA approaches include the combination of two neighborhood
37 methods namely the canonical correlation analysis (CCA) and the region of influence
38 (ROI) with two regional estimation (RE) models which are the log-linear regression
39 model (LLRM) and the generalized additive model (GAM). The RE models are also
40 applied without the hydrological neighborhood. Results show that regional models using
41 the extended dataset lead to significantly better flood quantile predictions, especially for
42 large basins. Indeed, the variable selection performed with EXTD consistently includes
43 some of the new variables, in particular the drainage density, the stream length ratio, and
44 the ruggedness number. Two other new variables are also identified and included in the
45 DHR step: the circularity ratio and the texture ratio. This leads to better predictions with
46 relative errors about 29% for EXTD, versus around 42% for STA in the case of the best

47 combination of RFA approaches. Thus, the proposed new variables allow for a better
48 representation of the physical dynamics within the watersheds.

49 **Keywords :** Drainage network characteristics; Ungauged basin; Canonical correlation
50 analysis; Region of influence; Generalized Additive Model, Regional frequency analysis.

51

52

53

54

55

56

57

58

59

60

61

62

63

64

65 **Abbreviations**

BH	Basin relief
BIAS	Mean bias
CCA	Canonical correlation analysis
DD	Drainage density
DDBZ	Mean annual degree days below 0 °C
DEM	Digital elevation model
DHR	Delineation of homogenous regions
Edf	Estimated smooth degree of freedom
EXTD	Extended dataset
FS	Stream frequency
GAM	Generalized additive model
IF	Infiltration number
LATC	Latitude of the centroid of the basin
LLRM	Log-linear regression model
LONGC	Longitude of the centroid of the basin
LU	Stream length
MALP	Mean annual liquid precipitation
MASP	Mean annual solid precipitation
MATP	Mean annual total precipitation
MBS	Mean basin slope
MCL	Main channel length
MRB	Mean bifurcation ratio
MRL	Mean stream length ratio
NASH	Nash efficiency criterion
NHN	National Hydro Network
PFOR	Percentage of the area occupied by forest
PLAKE	Percentage of the area occupied by lakes
PL1	Percentage of first-order stream lengths
PN1	Percentage of first-order streams
QS _T	Specific quantile associated to the return period T
Q _T	At-site flood quantile corresponding to return period T
R ²	Coefficient of determination
RB	Bifurcation ratio
RBIAS	Relative mean bias
RC	Circularity ratio
RE	Regional estimation
RFA	Regional frequency analysis
RL	Stream length ratio
RMSE	Root-mean-square error
RN	Ruggedness number
ROI	Region of influence
RRMSE	Relative root-mean-square error
RT	Texture ratio
STA	Standard dataset
U	Stream order
Var	Explanatory variable
WMRB	Weighted mean bifurcation ratio
ρ	RHO coefficient
ρ _{WMRB}	RHO WMRB coefficient

67 **1. Introduction**

68 Regional frequency analysis (RFA) procedures are commonly used in hydrology to
69 estimate flood and low-flow quantiles at sites where little or no hydrological data is
70 available. Generally, RFA includes two main steps: delineation of homogenous regions
71 (DHR) and regional estimation (RE) (e.g. Chebana et al. 2014; Chebana and Ouarda
72 2007; Ouarda 2016). In this context, climatic, morphometric and physiographic
73 characteristics of the watershed are widely used to describe geomorphic processes (e.g.
74 Baumgardner 1987; Hadley and Schumm 1961; Marchi and Dalla Fontana 2005;
75 Trambly et al. 2010) in order to predict hydrological variables using RFA approaches
76 (e.g. Dawson et al. 2006; Dodangeh et al. 2014; Goswami et al. 2007; Seidou et al. 2006;
77 Tsakiris et al. 2011).

78 A number of physio-meteorological variables, such as basin area, basin slope,
79 precipitation characteristics and land occupation are commonly used in the field of
80 hydrology and more precisely in the RFA procedures. They are considered as the most
81 relevant variables for these studies based on their high correlation with the hydrological
82 variables (Chokmani and Ouarda 2004). In addition to the commonly considered
83 variables (a more exhaustive list is in Table 1), drainage network characteristics (Jung et
84 al. 2017) and tectonic setting (e.g. Ahmadi et al. 2006; Hamed et al. 2014) may have a
85 strong impacts on hydrological dynamics, and are consequently related to flood quantiles.
86 However, they are not yet well investigated and integrated in RFA studies. Indeed, the
87 assessment of morphometric and physiographic variables requires the analysis of a
88 number of stream characteristics (e.g. ordering of the streams, bifurcation ratio, texture
89 ratio, stream length ratio, etc.). These variables characterize the basin shape as well as the

90 drainage system, and can be useful to model the hydrological dynamics. Youssef et al.
91 (2011) also indicated that the circularity ratio, number of orders and drainage density
92 have a direct impact on the hydrological risk. Hence, the integration of these variables in
93 the procedures for the regionalization of extreme hydrological events may contribute to
94 the enhancement of RFA results. Variables related to drainage network systems are
95 already used in several morphometric and hydrologic studies (e.g. Ameri et al. 2018;
96 Biswas et al. 1999; Kaliraj et al. 2015; Pareta and Pareta 2011; Rai et al. 2017; Ratnam et
97 al. 2005; Reddy et al. 2004; Sivasena Reddy and Janga Reddy 2013; Vijith and Satheesh
98 2006; Youssef et al. 2011) and they can eventually be useful in regionalization studies.
99 These variables can be extracted based on classical approaches such as topographic maps
100 and field examination or with advanced techniques using remote sensing and Digital
101 Elevation Models (DEM). Remote sensing techniques coupled with the potential of GIS
102 tools are increasingly popular. Indeed, they make it possible to calculate the various
103 characteristics of the basin very quickly and more efficiently based on a DEM which is
104 not possible in the past.

105 During the last decades, the focus in RFA has been mainly on the development of
106 new delineation and estimation methods (e.g. Durocher et al. 2015; Ouali et al. 2016;
107 Wazneh et al. 2016). Meanwhile, the list of physiographical and meteorological variables
108 used as predictors has seen little evolution. In the present study, a number of commonly
109 used RFA approaches are applied to test and evaluate the potential improvements that
110 may result from the adoption of new physiographic variables.

111 The objective of this work is to propose the use of new physiographical variables
112 related to the basin shape and drainage network and argue about their usefulness. To

113 evaluate their added value for quantile prediction in RFA, they are computed and used for
114 a set of 151 basins in Quebec (Canada). More specifically, the objective is to use both the
115 standard and extended databases to predict quantiles associated to several return periods,
116 and compare their prediction performances. In this work, standard RFA methods are
117 considered for quantile prediction, namely Canonical correlation analysis (CCA) (Ouarda
118 et al. 2000) and the region of influence (ROI) (Burn 1990) for DHR, including a case
119 with no DHR, as well as the log-linear regression model (LLRM) and the generalized
120 additive model (GAM) (Hastie 1986) for RE.

121 The present paper is structured as follows: Section 2 offers a review of the new
122 physiographic and morphometric variables proposed in this work by detailing their
123 characteristics. Section 3 briefly presents the theoretical background of the CCA and the
124 ROI approaches for the delineation of neighborhoods and the LLRM and the GAM for
125 the regional estimation. The adopted methodology and the developed regional models are
126 detailed in section 4. Section 5 describes the study area and the used datasets. The results
127 are presented and discussed in section 6, and the conclusions of the work are summarized
128 in the last section.

129 **2. Variables characterizing drainage networks**

130 Drainage network characteristics and evolution depend closely on the prevailing
131 climatic, physiographic, and topographic conditions of the basin (Jung et al. 2015). These
132 conditions determine the drainage network configuration which, in turn, can affect the
133 hydrological response of the watershed (Howard 1990), and consequently hydrological
134 quantile estimation. The new physiographical variables considered in this work are

135 presented herein. Table 2 summarizes the definitions and standard mathematical
136 equations used to determine these variables.

137 **2.1 Stream order (*U*)**

138 The stream order of a basin is the highest stream order within the basin, where an
139 order one is a stream starting at the source. A number of stream ordering systems are
140 available in the hydrological literature. The simplest and most used one is the Strahler
141 system originally introduced by Horton (1945) and then modified by Strahler (1952).
142 This method is based on a hierarchical ranking of streams. When two first order streams
143 join, an order two is formed and so on. Several researchers have directly correlated the
144 stream order with stream flow (e.g. Blyth and Rodda 1973; Stall and Fok 1967). Blyth
145 and Rodda (1973) also observed that during dry periods, first-order streams present less
146 than 20% of the total length of the drainage network. At the maximum development of
147 the drainage network, the total length of first-order streams constitutes over 50% of the
148 total basin stream length. Thus, stream order frequency, especially the frequency of the
149 first-order streams, may be well correlated with the hydrological response of the
150 watershed.

151 **2.2 Texture ratio (*RT*)**

152 The texture ratio (*RT*) allows characterizing the basin drainage texture and is one of
153 the most important factors in the drainage morphometric analysis due to its high
154 relationship with the underlying lithology, the infiltration ability and the topographic
155 characteristics of the terrain (Schumm 1956). High *RT* levels indicate the presence of soft

156 rocks with high sensitivity to erosion (Ameri et al. 2018), and consequently a high and
157 speedy surface runoff.

158 **2.3 Circularity ratio (*RC*)**

159 The circularity ratio (*RC*) is defined as the ratio between the areas of a catchment to
160 the area of the circle having the same perimeter of the catchment. It is an important
161 variable that helps characterize the basin shape. It is affected by the length and frequency
162 of streams, geological structures, land use and cover, and the slope of the catchment (Dar
163 et al. 2014; Vijith and Satheesh 2006). *RC* values range between 0 and 1. Basins with *RC*
164 values close to 1 are characterized by circular form and a low concentration time and then
165 a high peak flow. Low *RC* values are associated with strongly elongated basins and with
166 lower runoff.

167 **2.4 Stream length ratio (*RL*)**

168 The stream length ratio (*RL*) was defined by Horton (1945) as the ratio between the
169 mean length of the streams of a given order and the next lower order. It is based on
170 Horton's law (1945) of stream length that indicates the existence of a direct geometric
171 relationship between the mean length of the streams of a given order and the next lower
172 order. The *RL* between successive stream orders changes under the effect of the
173 topographic and slope variability, and has a significant relationship with surface runoff
174 and the erosional stage of the watershed (Sreedevi et al. 2005).

175 **2.5 Mean bifurcation ratio (*MRB*) and weighted mean bifurcation ratio (*WMRB*)**

176 The bifurcation ratio (*RB*) is defined as the ratio between the stream's number of a
177 given order and those of the next-higher order in a drainage network. It permits the
178 characterization of the impacts of the geological structures on the drainage network.
179 Strahler (1957) indicated that the *RB* shows a slight range of variation for different
180 regions except where the impact of the geological control is important. Chow (1964),
181 Strahler (1964) and Verstappen (1983) indicated that, in general, the geological structures
182 have a negligible impact on drainage networks, if the mean bifurcation ratio (*MRB*) of the
183 watershed is comprised between 3 and 5. A higher value of this variable indicates a sort
184 of geological control (Agarwal 1998). This variable can also characterize the watershed's
185 shape. A high *RB* value is, generally, associated with an elongated basin, while a low *RB*
186 value is likely to be associated with a circular basin (Gajbhiye 2015; Taofik et al. 2017).
187 Strahler (1953) proposed a more representative bifurcation number measure, called
188 weighted mean bifurcation ratio (*WMRB*). It consists in multiplying the ordinary *RB*
189 identified for each successive order by the total number of streams involved in the ratio
190 and subsequently taking the mean of these values. Schumm (1956) used this approach to
191 determine the *WMRB* of the drainage system of the Perth Amboy (N.J). Pareta and Pareta
192 (2011) and Bajabaa et al. (2014) also used this variable in hydrologic and morphometric
193 analysis studies.

194 **2.6 RHO coefficient (ρ)**

195 The RHO coefficient (ρ) is defined as the ratio between the *RL* and the *RB* of the
196 watershed. It characterizes the relationship between the physiographic development of
197 the watershed and the drainage density, and permits the assessment of the storage

198 capacity of the drainage network (Horton 1945). This variable is affected by several
199 climatic, geologic, biologic, geomorphologic and anthropogenic factors (Mesa 2006).

200 **2.7 Drainage density (*DD*)**

201 The drainage density (*DD*) was introduced by Horton (1932) in the hydrological
202 literature as the total length of stream networks per unit area. *DD* express the closeness of
203 the spacing of streams, and provides a quantitative measurement of landscape dissection
204 and runoff potential (Magesh et al. 2011). It is a result of interacting factors controlling
205 the surface runoff such as, the infiltration capacity, the climatic conditions and the
206 vegetation cover of the watershed (Máčka 2001; Patton 1988; Reddy et al. 2004;
207 Verstappen 1983).

208 **2.8 Stream frequency (*FS*)**

209 The stream frequency (*FS*) is the number of stream segments of all orders per unit
210 area (Horton 1932; Horton 1945). It depends on the rock characteristics, infiltration
211 capacity, vegetation cover, relief, amount of rainfall and subsurface permeability (Hajam
212 et al. 2013), and reflects the texture of the drainage network (Magesh et al. 2011). In
213 general, a high *FS* is associated with impermeable subsurface, sparse vegetation, high
214 relief conditions and low infiltration capacity (Reddy et al. 2004; Shaban et al. 2005).

215 **2.9 Infiltration number (*IF*)**

216 The infiltration number (*IF*) is defined by Faniran (1968) as the product of the *DD*
217 and the *FS*. It allows the characterization of the watershed infiltration capacity (Hajam et
218 al. 2013). This variable is inversely proportional to the infiltration capacity of the basin.

219 The higher the IF values, the lower will be the infiltration and the higher will be the
220 runoff (Pareta and Pareta 2011).

221 **2.10 Ruggedness number (RN)**

222 The ruggedness number (RN) is often used to evaluate the flood potential of
223 streams (Patton and Baker 1976) and it usually combines the impact of slope steepness
224 with its length (Strahler 1964). This variable allows describing the structural complexity
225 of the terrain. Watersheds characterized by high RN values are highly subject to erosion
226 and therefore susceptible to an increased peak flow (Sreedevi et al. 2013).

227 **3. Theoretical background**

228 In this section, we briefly present the statistical approaches adopted in the present
229 work. We define a RFA model as a two-step procedure beginning with a neighborhood
230 identification method and then performing regional estimation. We hereby consider two
231 different methods for each step, which are described below.

232 **3.1 Delineation of homogeneous regions**

233 **3.1.1 Canonical correlation analysis (CCA)**

234 CCA method is detailed in Ouarda et al. (2001) in the context of RFA, and
235 commonly used in this context to identify group of basins having the same hydrological
236 response. This method consists of space reduction by establishing pairs of canonical
237 variables based on a linear transformation of two groups of random variables. Let two
238 sets of random variables $X=(X_1, X_2, \dots, X_m)$ and $Y=(Y_1, Y_2, \dots, Y_n)$ containing,
239 respectively, the m physio-meteorological variables and the n hydrological variables of N

240 gauged sites. Based on these variables, the linear combinations V_i and Z_i of the variables
241 X and Y and the canonical correlation coefficients $\lambda_1, \dots, \lambda_p$ (with $\lambda_i = \text{corr}(V_i, Z_i)$) can
242 be computed.

243 Using the CCA method, the considered basins can be represented as points in a spaces of
244 the uncorrelated canonical variables (V_i, Z_j) ; where $i \neq j$. Then, it will be possible to
245 examine the similarity of the point patterns in these spaces, i.e., the ability of the physio-
246 meteorological canonical variables to predict the hydrological variables. The point
247 patterns that are sufficiently similar are associated with sub-group of basins that belongs
248 to the same statistical population and vice versa. The similarity between the basins are
249 measured based on a Mahalanobis distance.

250 **3.1.2 Region of influence (ROI)**

251 As the CCA, the ROI method (Burn 1990) allows the identification of a
252 hydrological neighborhood for a given target-site based on a Euclidean distance,
253 generally a weighted Euclidean distance. This distance determines the similarity of
254 watersheds in a multidimensional space of physio-meteorological variables. A more
255 detailed description of the approach can be found for example in Burn (1990) and
256 GREHYS (1996).

257 **3.2 Regional estimation approaches**

258 **3.2.1 Linear Regression Model**

259 The linear regression model or the log-linear regression model (LLRM) is commonly
260 used to find a linear relationship between the hydrological variable (such as the flood
261 quantile Q_T corresponding to a return period T) and the physio-meteorological

262 characteristics of a watershed (X_1, X_2, \dots, X_m), and it is defined as (e.g. Girard et al.
263 2004; Pandey and Nguyen 1999) :

$$\log (E(Y/X))= \beta_0 + \sum_{j=1}^m \beta_j \log (X_j) + \varepsilon \quad (1)$$

264 where X is a matrix whose columns correspond to a set of m explanatory variables, β_0
265 and β_j are unknown parameters to be estimated using the least-square method (Pandey and
266 Nguyen 1999) and ε is the model error.

267 **3.2.2 Generalized Additive Model**

268 GAM was developed by Hastie and Tibshirani (1986). It is an extension of the
269 generalized linear model (GLM). This model allows for a response distribution other than
270 Gaussian and for a non-linear relationship between response and explanatory variables
271 through smooth functions (Hastie 1986; Wood 2006), which may lead to a more close
272 description of the hydrological processes involved. The GAM formula is given by Wood
273 (2006):

$$g (E(Y/X))= \beta_0 + \sum_{j=1}^m S_j (X_j) + \varepsilon \quad (2)$$

274 where g is a monotonic link function and S_j are smooth functions of explanatory
275 variables X_j .

276 The estimation of the smooth functions S_j is carried out using splines, which are
277 piecewise polynomial functions linked at points named knots. Generally, the smooth
278 functions S_j are defined as follows:

$$S_j(x) = \sum_{i=1}^q \beta_{ji} b_{ji}(x) \quad (3)$$

279 where β_{ji} are unknown parameters and b_{ji} are the spline basis functions.

280 4. Methodology

281 4.1 Regional models

282 In this study, we apply all combinations of the two DHR methods (CCA, ROI) in
283 conjunction with the RE models (LLRM and GAM) presented in section 3. The RE
284 models are also considered with all stations (i.e. without defining any neighborhood).
285 This result in six possible combinations for each dataset (STA and EXTD). Thus, the
286 following regionalization approaches are evaluated (Fig.1):

- 287 • ALL/LLRM (STA and EXTD): LLRM used without neighborhoods (all stations) and
288 with variables selected from the STA and the EXTD datasets using the backward
289 stepwise procedure.
- 290 • ALL/GAM (STA and EXTD): GAM used without neighborhoods (all stations) and
291 with variables selected from the STA and the EXTD datasets using the backward
292 stepwise procedure.
- 293 • CCA/LLRM (STA and EXTD): LLRM used with neighborhoods identified by the
294 CCA method and with variables selected from the STA and the EXTD datasets using
295 the backward stepwise procedure.

- 296 • CCA/GAM (STA and EXTD): GAM used with neighborhoods identified by the CCA
297 method and with variables selected from the STA and the EXTD datasets using the
298 backward stepwise procedure.
- 299 • ROI/LLRM (STA and EXTD): LLRM used with neighborhoods identified by the ROI
300 method and with variables selected from the STA and the EXTD datasets using the
301 backward stepwise procedure.
- 302 • ROI/GAM (STA and EXTD): GAM used with neighborhoods identified by the ROI
303 method and with variables selected from the STA and the EXTD datasets using the
304 backward stepwise procedure

305 The CCA and ROI methods are used in the DHR considering two different sets of
306 physio-meteorological variables. The first group includes variables from the STA dataset,
307 namely the area (AREA), mean basin slope (MBS), percentage of the area occupied by
308 lakes (PLAKE), mean annual total precipitation (MATP), mean annual degree days
309 below 0 °C (DDBZ) and the longitude of the centroid of the catchment (LONGC). The
310 second one comprises variables from the EXTD dataset, which are PLAKE, MATP,
311 DDBZ, LONGC, *RT* and *RC*. The selection of these variables is carried out based on their
312 correlation level with the hydrological variables (Table 3) as the principle of the CCA is
313 based on correlations. For the aim of simplicity and to be consistent with the CCA,
314 variables selected for the ROI are also based on correlation levels.

315 The classical procedures of ROI and CCA lead to neighbourhoods with highly
316 variable sample sizes from a target site to another. Indeed, considering a given threshold
317 value, sites located near the centre of the cloud of points determined by the Euclidean
318 space for ROI and the canonical space for CCA are expected to include more sites within

319 their neighbourhoods than sites located on the edge of the cloud of points (Leclerc and
320 Ouarda 2007). Since the accuracy of the estimates obtained by regression models is
321 sensible to the sample size, it was decided to fix the neighbourhood size for all target
322 stations. This size is chosen with a standard jackknife procedure and optimized using the
323 optimization procedure of Ouarda et al. (2001) developed in the Matlab environment.

324 LLRM and GAM are used in this study as RE models. GAM was developed based
325 on the R package mgcv (Wood 2006). In this work, the thin plate regression spline is
326 considered as basis $b_{ji}(\cdot)$ in the smoothing function $S_j(\cdot)$ in equation (3). This basis
327 function is considered due to its advantages. The thin plate regression spline is
328 characterized by its reduced calculation time, its flexibility and it comprises a lower
329 number of parameters compared to other smoothing functions (Wood 2006). The
330 considered link function g in (2) is the identity function since the log-transformed
331 quantiles are approximately normal (as in Ouali et al. (2017)).

332 4.2 Selection of explanatory variables

333 Variable selection procedure is different for the two RFA steps; a correlation-based
334 selection is considered for DHR and a stepwise method is used for RE as a standard
335 approach in the RFA studies. Based on correlation level between physio-meteorological
336 variables and hydrological variables (Table3), six variables are identified for DHR (see
337 above).

338 For the RE step, four variable selection methods are firstly tested namely forward,
339 backward, stepwise and shrinkage approaches (Heinze et al. 2018) in this study. Table 4
340 presents the results obtained from each variable selection approach applied for QS_{10} that

341 can be considered as the most reliable quantile. It can be seen that, regardless of the
342 considered selection method, several new variables are selected in the final model. This
343 suggests that new variables in the EXT-D are potentially useful for RFA.

344 To evaluate whether the new variables are predictive of target quantiles, the
345 backward stepwise selection procedure is adopted for both LLRM and GAM. It has
346 already been successfully applied previously with the same dataset (STA) and in the
347 same context by Chebana et al. (2014), Ouarda et al. (2018) and more recently by Msilini
348 et al. (2020). Backward stepwise selection procedure consists in a progressive elimination
349 of variables having the highest p value (based on the hypothesis that the coefficients in
350 equation (1) for LLRM or the smooth terms in equation (3) for GAM are null) from an
351 initial model comprising all available variables. The procedure stops when the number of
352 variables remaining in the model drops below a specific number (Fig.2). This number is
353 chosen as the one minimizing the RRMSE estimated by jackknife.

354 **4.3 Models validation**

355 For each RFA model, a jackknife procedure (also called leave one-out cross
356 validation procedure) is used to evaluate its performance. It consists in considering, in
357 turn, each gauged site as an ungauged one and comparing thereafter the regional estimate
358 to the observed value. This comparison is performed through several criteria: first, the
359 Nash criterion (NASH) gives an evaluation of the degree of adequacy and a global
360 assessment of the prediction quality. Second, the root mean squared error (RMSE)
361 provides information about the accuracy of the prediction in an absolute scale, and the
362 relative RMSE (RRMSE) removes the impact of each site's order of magnitude from the

363 RMSE values and gives information about the accuracy of the prediction in a relative
 364 scale. Finally, the bias (BIAS) and the relative bias (RBIAS) give a measure of the
 365 magnitude of the systematic overestimation or underestimation of a model. The
 366 formulations of these criteria are given as follows:

Nash:

$$\text{NASH} = 1 - \frac{\sum_{i=1}^N (y_i - \hat{y}_i)^2}{\sum_{i=1}^N (y_i - \bar{y})^2} \quad (4)$$

Root-mean-square error :

$$\text{RMSE} = \sqrt{\frac{1}{N} \sum_{i=1}^N (y_i - \hat{y}_i)^2} \quad (5)$$

Relative root-mean-square error :

$$\text{RRMSE} = 100 \sqrt{\frac{1}{N} \sum_{i=1}^N \left[\frac{(y_i - \hat{y}_i)}{y_i} \right]^2} \quad (6)$$

Mean bias :

$$\text{BIAS} = \frac{1}{N} \sum_{i=1}^N (y_i - \hat{y}_i) \quad (7)$$

Relative mean bias :

$$\text{RBIAS} = 100 \frac{1}{N} \sum_{i=1}^N \frac{(y_i - \hat{y}_i)}{y_i} \quad (8)$$

367 where y_i and \hat{y}_i are, respectively, the local and regional quantile estimates at site i , \bar{y} is
 368 the mean of the local quantile estimates, and N is the number of stations.

369 5. Case study and datasets

370 The data used in this study includes two datasets, the STA and the EXTD, covering
371 151 stations located in the southern part of Quebec, Canada (Fig. 3). The STA was
372 considered in previous studies with geographical coordinates of the stations and
373 commonly used physio-meteorological variables (e.g. Durocher et al. 2015; Shu and
374 Ouarda 2007; Wazneh et al. 2016). The EXTD dataset combining STA dataset with less
375 common variables representing drainage network properties. The stations are operated by
376 the Ministry of Sustainable Development, Environment, and Fight Against Climate
377 Change.

378 The considered hydrological variables (Y in the theoretical background) are at-site
379 quantiles standardized by the basin area (specific quantiles), denoted by QS_{10} , QS_{50} and
380 QS_{100} with 10, 50 and 100 are the return periods. Descriptive statistics of hydrological
381 and physio-meteorological variables of the STA (not presented here to avoid repetition)
382 can be found for example in Durocher et al. (2015). The hydrological variables were
383 identified in Kouider et al. (2002a) using a local Frequency Analysis in each gauged site.
384 Data series with at least 15 years of measurement were considered for the analysis. The
385 basic assumptions of stationarity, homogeneity and independence were verified and the
386 appropriate statistical distributions were fitted to data. The appropriate probability
387 distributions identified, are mainly the inverse gamma and Log-Normal with two
388 parameters. For more details about this study, reader may refer to the report of Kouider et
389 al. (2002b). The new physiographical variables, considered in the EXTD, are summarized
390 in Table 5. These variables are identified from drainage networks extracted using the D8
391 method based on the DEMs (Jenson and Domingue 1988; O'Callaghan and Mark 1984).
392 This technique is implemented in Arc Gis (Arc Hydro).

393 The D8 method is based on a digital elevation model (DEM) which is basically a
394 grid of elevation values. For each cell, it is considered that water flows in direction of the
395 steepest slope among the eight neighbors of a given DEM cell. The direction grid can
396 then be used to estimate flow accumulation which is obtained by summing the weight of
397 all grid cells following into each downslope cell in the output grid, i.e. simulating the
398 flow path. Based on the obtained flow accumulation grid, the drainage networks can be
399 extracted with the stream head locations corresponding to accumulation values below a
400 constant threshold value (see for instance (Tarboton et al. 1991)).

401 In this work, the DEMs were hydrologically corrected based on information from the
402 National Hydro Network (NHN). This correction was carried out using the DEM
403 Reconditioning process, which is an implementation of the “AGREE” method. It consists
404 in adjusting the DEM by imposing linear features as a reference. The reference in this
405 case is the (NHN).

406 The used DEMs have a spatial resolution of ~ 20 m grid cells and are obtained from
407 the Natural Resources Canada database ([https://www.nrcan.gc.ca/earth-
408 sciences/geography/topographic-information/download-directory-documentation/17215](https://www.nrcan.gc.ca/earth-sciences/geography/topographic-information/download-directory-documentation/17215)).
409 Note that, drainage networks of six cross-border watersheds are extracted using the
410 United States Geological Survey (USGS) data distributed with ~ 30 m grid cells
411 (<https://earthexplorer.usgs.gov/>).

412 CCA requires the normality of all variables. Hence, some variables need to be
413 transformed. The normality of each variable is visually assessed with a normal
414 probability plot. This technique plots empirical quantiles versus theoretical Gaussian

415 quantiles and should be approximately linear in the case of actual normality. The
416 logarithmic transformation is considered for the hydrological variables, AREA, MBS,
417 MATP, DDBZ and *RT*, and a square root transformation for PLAKE and *RC*. The
418 LONGC is used without transformation since it is approximately normal.

419

420 **6. Results and Discussion**

421 A correlation analysis is carried out in order to investigate the relationships
422 between variables. Table 3 shows the list of the variables selected for the DHR step based
423 on their high correlation level with the hydrological variables. One can see the existence
424 of relatively high negative correlations between the hydrological variables and the
425 AREA, PLAKE, DDBZ and *RT*. We also note the presence of important positive
426 correlations between the response variables and the MATP and *RC* variables. The linear
427 correlation coefficients between the variable *RT*, which is one of the most important new
428 variables, and the specific quantiles QS_{10} and QS_{100} are -0.53 and -0.51 respectively.
429 However, those between the *RT* variable and the at-site flood quantiles Q_{10} and Q_{100} are
430 0.87 and 0.86 respectively. Positive and high correlation values indicate that the increase
431 in *RT* is associated with a relatively fast and high hydrologic response and consequently
432 an increased risk of erosion. This is consistent with what is stated in Ameri et al. (2018).
433 The second important new variable in terms of correlation level is the *RC* characterizing
434 the basin shape. Higher *RC* values (close to 1) are associated with circular basins with
435 low concentration time and high hydrological response hence the positive correlation.

436 The identification of the neighborhood requires the determination of the optimal
437 number of stations to be used in the RE step. To this end, the optimization procedure of
438 Ouarda et al. (2001) is used. Based on a selected criterion such as RMSE, RRMSE, BIAS
439 or RBIAS the optimal size of neighborhoods can be identified. The optimal size of the
440 neighborhoods should be large enough to ensure that RE can be carried out effectively,
441 but not too large in order to maintain an acceptable degree of homogeneity within the
442 neighborhoods. In this study, we obtain $n^{\text{opt}}(\text{STA}) = 85$ sites and $n^{\text{opt}}(\text{EXTD}) = 78$ sites
443 with respect to the RRMSE, which is the most important criterion (Hosking and Wallis
444 2005), for the CCA approach. For the ROI method, the obtained optimum sizes are n^{opt}
445 (STA) = 54 sites and $n^{\text{opt}}(\text{EXTD}) = 44$ sites with respect to the same criterion.

446 The backward stepwise selection method is considered for each quantile (QS₁₀, QS₅₀
447 and QS₁₀₀) and for each model (LLRM and GAM). In the present study, the optimal
448 number of variables in GAM, which is the most complex model, is found to be seven.
449 Table 6 shows the seven selected variables for each quantile and model combination. We
450 note the selection of three new variables (*RN*, *MRL* and *DD*).

451 The jackknife procedure results for all considered combinations are presented in
452 Table 7. The best overall performances are obtained with the EXTD, especially with
453 ROI/GAM/EXTD followed by the CCA/GAM/EXTD approaches. Based on the high
454 NASH values (0.79) and the lowest RRMSE values (29.24 % for QS₁₀₀), the
455 ROI/GAM/EXTD combination gives the most precise estimates compared to all other
456 approaches. According to RBIAS, all models underestimate flood quantiles but the least
457 biased model is ROI/LLRM/EXTD (-1.38 % for QS₁₀₀). However, compared to the
458 ROI/GAM/EXTD approach, the difference is low (around -1.8 % for QS₁₀₀).

459 Note that, GAM applied to EXTD (with and without the neighborhoods) outperforms
460 LLRM applied to EXTD and STA. This may be explained by the ability of GAM to take
461 into account the possible nonlinear connections between predictor and response variables,
462 and also by the important impact of the new variables.

463 We also notice that the use of the EXTD leads to even more important improvements
464 when adopting the ROI method compared to the CCA approach. Wazneh et al. (2016)
465 have also obtained better results with the ROI than with the CCA approach.

466 To further explain the previous results, the relative errors as a function of the stations
467 ordered according to their area corresponding to the best combinations (ROI/GAM and
468 CCA/GAM) are given in Fig. 4 and Fig. 5 respectively. It can be seen that the EXTD
469 performs well especially for large basins. Indeed, for the large watersheds the relative
470 errors decrease considerably with the EXTD. This result may also be confirmed by Fig. 6,
471 where one can note that the lowest specific quantiles, which are usually associated to
472 sites with large basin areas, are well estimated with the EXTD. A significant
473 improvement can also be seen for some specific sites that have exceptionally large
474 relative errors with STA. Four such sites (030401, 030402, 041903 and 042607) were
475 identified previously by Chokmani and Ouarda (2004), Durocher et al. (2015) and Ouali
476 et al. (2017) as particular stations with underestimated areas. The integration of more
477 accurate variables dealing with the drainage network, improves considerably the quantile
478 estimates corresponding to these sites.

479 Jackknife estimates using the ROI/GAM and CCA/GAM approaches (for QS_{100}) are
480 illustrated, respectively, in Fig. 7 and Fig. 8. One can see that these models combined
481 with the EXTD show better performances compared to the STA. The points associated to

482 the scatter diagram of the at-site and regional estimates are less dispersed when using the
483 EXTD than the STA. In addition, the coefficient of determination R^2 values show that the
484 linearity between the local and the regional specific quantile estimates is better explained
485 when using the EXTD than the STA.

486 Results also indicate that sites with high specific quantile values (more than 0.7
487 $\text{m}^3/\text{s.km}^2$), which are generally associated to small basins with an area less than 800 km^2 ,
488 are underestimated using the two datasets. This may suggest the usefulness of developing
489 specific regional models for small basins. This result can be explained by the fact that
490 traditional neighborhood approaches (CCA and ROI) lead to an underestimation for sites
491 with small basin areas as shown in Wazneh et al.(2016). This may be the cause of the
492 obtained negative RBIAS values in this work.

493 Fig. 9 and Fig. 10 present the smooth functions of the response variable $\log(\text{QS}_{100})$ as
494 a function of the STA and the EXTD explanatory variables respectively. We notice that
495 the variables PLAKE, DDBZ, AREA and *DD* show a complex nonlinear relationship
496 (nonlinear smooth function curves and high edf values), while the variables LONGC;
497 MALP, MCL, MBS and *MRL* present linear relations.

498 A particular case of interest from the EXTD that can be observed concerns the
499 relationship between the hydrological variable and the *DD* values. One can see that the
500 higher the *DD* values are the lower the hydrological response will be. This result is in
501 contradiction with what is commonly observed in practice (Melton 1957). In fact, the
502 correlation between the *DD* variable and specific quantile is negative (-0.11) while the
503 correlation between flood quantile and the variable *DD* is positive (0.13). Thus, this

504 variable depends on the size of the watershed, for this reason its effect is reversed in this
505 study case because the specific quantile is used.

506 We also notice that the *MRL* and *MCL* variables are found to be inversely
507 proportional to the hydrological response. An increase of these variables is associated
508 with a decrease of the *MBS* and hence a decrease of the hydrological response.

509 It can also be seen that the relationship between $\log(QS_{100})$ and *PLAKE* is decreasing
510 for the majority of *PLAKE* values, but increases for the highest values of *PLAKE*.
511 However, the number of points is very limited in the high *PLAKE* range and more effort
512 will be required to understand the effect of this variable on the flow regime for this range.
513 In general, lakes act as a sponge absorbing the excess water during extreme events, which
514 explains the decreasing relationship between $\log(QS_{100})$ and *PLAKE*.

515 The *LONGC* in this study is an indicator of the station proximity to the Atlantic
516 Ocean and thereafter reflects the influence of the ocean on the local climate. Finally, the
517 variability in the relationship between the *DDBZ* values and the hydrological response
518 may indirectly reflect the seasonality impact of the temperature on the flow regime. The
519 same patterns were observed previously by Chebana et al. (2014) for the *DDBZ* and
520 *PLAKE* variables.

521 **7. Conclusions**

522 Through a case study in the province of Quebec, the present study shows the
523 relevancy of considering drainage network characteristics for quantile prediction in RFA.
524 This result is outlined by the variable importance in RFA models which shows that five

525 new variables, namely RT, RC, DD, MRL and RN are found particularly useful for the
526 specific case of Quebec. Prediction accuracy is also improved using the new variables,
527 especially when considering small neighbourhoods and nonlinear models as shown by the
528 superior accuracy of the ROI/GAM/EXTD combination. This result seems also more
529 important for large basins.

530 By focusing on the drainage network and basin shape, the new geographical
531 variables allow integrating more information about the underlying hydrogeological flows
532 and thus, indirectly, to make the link between the groundwater and the surface water
533 flows. This added information allows for a better description of the hydrological
534 dynamics involved and consequently to better flood quantile estimates.

535 The present study paves the way for several perspectives. In particular, drainage
536 network characteristics should be evaluated further in a wider variety of settings
537 including different climate and catchment geology. The increasing complexity of
538 databases used in RFA to which this research participate, also outlines the need for
539 methodological development that allow a more efficient use of this extensive
540 information, as classical approaches may be limited in this regard. Future research should
541 thus focus on studying how to take advantage of the interaction between the newly
542 proposed variables on quantile estimation, as well as the potential nonlinear impact of the
543 considered variables.

544

545

546

547 **References**

- 548 Agarwal C (1998) Study of drainage pattern through aerial data in Naugarh area of Varanasi
549 district, UP Journal of the Indian Society of Remote Sensing 26:169-175
550 doi:<https://doi.org/10.1007/BF02990795>
- 551 Ahmadi R et al. (2006) The geomorphologic responses to hinge migration in the fault-related
552 folds in the Southern Tunisian Atlas Journal of Structural Geology 28:721-728
- 553 Alobaidi MH, Marpu PR, Ouarda TB, Chebana F (2015) Regional frequency analysis at
554 ungauged sites using a two-stage resampling generalized ensemble framework Advances
555 in Water Resources 84:103-111 doi:<https://doi.org/10.1016/j.advwatres.2015.07.019>
- 556 Ameri AA, Pourghasemi HR, Cerda A (2018) Erodibility prioritization of sub-watersheds using
557 morphometric parameters analysis and its mapping: A comparison among TOPSIS,
558 VIKOR, SAW, and CF multi-criteria decision making models Science of The Total
559 Environment 613:1385-1400 doi:<https://doi.org/10.1016/j.scitotenv.2017.09.210>
- 560 Aziz K, Rahman A, Fang G, Shrestha S (2014) Application of artificial neural networks in
561 regional flood frequency analysis: a case study for Australia Stochastic environmental
562 research and risk assessment 28:541-554
- 563 Bajabaa S, Masoud M, Al-Amri N (2014) Flash flood hazard mapping based on quantitative
564 hydrology, geomorphology and GIS techniques (case study of Wadi Al Lith, Saudi
565 Arabia) Arabian Journal of Geosciences 7:2469-2481 doi:<https://doi.org/10.1007/s12517-013-0941-2>
- 566
- 567 Baumgardner RW (1987) Morphometric Studies of Subhumid and Semiarid Drainage Basins,
568 Texas Panhandle and Northeastern New Mexico. vol 163. Bureau of Economic Geology,
569 University of Texas at Austin,
- 570 Beck HE, Dijk AI, Miralles DG, Jeu RA, McVicar TR, Schellekens J (2013) Global patterns in
571 base flow index and recession based on streamflow observations from 3394 catchments
572 Water Resources Research 49:7843-7863 doi:<https://doi.org/10.1002/2013WR013918>
- 573 Biswas S, Sudhakar S, Desai V (1999) Prioritisation of subwatersheds based on morphometric
574 analysis of drainage basin: A remote sensing and GIS approach Journal of the Indian
575 society of remote sensing 27:155-166 doi:<https://doi.org/10.1007/BF02991569>
- 576 Blyth K, Rodda J (1973) A stream length study Water Resources Research 9:1454-1461 doi:
577 <https://doi.org/10.1029/WR009i005p01454>
- 578 Burn DH (1990) Evaluation of regional flood frequency analysis with a region of influence
579 approach Water Resources Research 26:2257-2265 doi:
580 <https://doi.org/10.1029/WR026i010p02257>
- 581 Castellarin A (2014) Regional prediction of flow-duration curves using a three-dimensional
582 kriging Journal of hydrology 513:179-191
583 doi:<https://doi.org/10.1016/j.jhydrol.2014.03.050>
- 584 Castiglioni S, Castellarin A, Montanari A (2009) Prediction of low-flow indices in ungauged
585 basins through physiographical space-based interpolation Journal of hydrology 378:272-
586 280 doi:<https://doi.org/10.1016/j.jhydrol.2009.09.032>
- 587 Chebana F, Charron C, Ouarda TBMJ, Martel B (2014) Regional frequency analysis at ungauged
588 sites with the generalized additive model Journal of Hydrometeorology 15:2418-2428
589 doi:<https://doi.org/10.1175/JHM-D-14-0060.1>

590 Chebana F, Ouarda TB (2007) Multivariate L-moment homogeneity test Water resources research
591 43 doi:doi:10.1029/2006WR005639

592 Chokmani K, Ouarda TB (2004) Physiographical space-based kriging for regional flood
593 frequency estimation at ungauged sites Water Resources Research 40

594 Chow V (1964) Handbook of applied hydrology: a compendium of water-resources technology
595 vol 1. McGraw-Hill,

596 Dar RA, Romshoo SA, Chandra R, Ahmad I (2014) Tectono-geomorphic study of the Karewa
597 Basin of Kashmir Valley Journal of Asian Earth Sciences 92:143-156
598 doi:<https://doi.org/10.1016/j.jseaes.2014.06.018>

599 Dawson CW, Abrahart RJ, Shamseldin AY, Wilby RL (2006) Flood estimation at ungauged sites
600 using artificial neural networks Journal of hydrology 319:391-409
601 doi:<https://doi.org/10.1016/j.jhydrol.2005.07.032>

602 Dodangeh E, Soltani S, Sarhadi A, Shiau JT (2014) Application of L-moments and Bayesian
603 inference for low-flow regionalization in Sefidroud basin, Iran Hydrological Processes
604 28:1663-1676 doi:<https://doi.org/10.1002/hyp.9711>

605 Durocher M, Chebana F, Ouarda TB (2015) A nonlinear approach to regional flood frequency
606 analysis using projection pursuit regression Journal of Hydrometeorology 16:1561-1574
607 doi:<https://doi.org/10.1175/JHM-D-14-0227.1>

608 Faniran A (1968) The index of drainage intensity-A provisional new drainage factor Australian
609 Journal of Science 31:328-330

610 Flavell D (2012) Design flood estimation in Western Australia Australian Journal of Water
611 Resources 16:1-20

612 Gajbhiye S (2015) Morphometric analysis of a Shakkar river catchment using RS and GIS
613 International Journal of u-and e-Service, Science and Technology 8:11-24
614 doi:<http://dx.doi.org/10.14257/ijunesst.2015.8.2.02>

615 Girard C, Ouarda TB, Bobée B (2004) Étude du biais dans le modèle log-linéaire d'estimation
616 régionale. Canadian Journal of Civil Engineering 31:361-368
617 doi:<https://doi.org/10.1139/103-099>

618 Goswami M, O'connor K, Bhattarai K (2007) Development of regionalisation procedures using a
619 multi-model approach for flow simulation in an ungauged catchment Journal of
620 Hydrology 333:517-531 doi:<https://doi.org/10.1016/j.jhydrol.2006.09.018>

621 GREHYS (1996) Presentation and review of some methods for regional flood frequency analysis
622 Journal of hydrology(Amsterdam) 186:63-84

623 Griffis V, Stedinger J (2007) The use of GLS regression in regional hydrologic analyses Journal
624 of Hydrology 344:82-95 doi:<https://doi.org/10.1016/j.jhydrol.2007.06.023>

625 Haddad K, Rahman A (2012) Regional flood frequency analysis in eastern Australia: Bayesian
626 GLS regression-based methods within fixed region and ROI framework–Quantile
627 Regression vs. Parameter Regression Technique Journal of Hydrology 430:142-161
628 doi:<https://doi.org/10.1016/j.jhydrol.2012.02.012>

629 Hadley R, Schumm S (1961) Sediment sources and drainage basin characteristics in upper
630 Cheyenne River basin US Geological Survey Water-Supply Paper 1531:198

631 Hailegeorgis TT, Alfredsen K (2017) Regional flood frequency analysis and prediction in
632 ungauged basins including estimation of major uncertainties for mid-Norway Journal of
633 Hydrology: Regional Studies 9:104-126 doi:<https://doi.org/10.1016/j.ejrh.2016.11.004>

634 Hajam RA, Hamid A, Bhat S (2013) Application of morphometric analysis for geo-hydrological
635 studies using geo-spatial technology-A case study of Vishav Drainage Basin Hydrol
636 Current Res 4:2 doi:<http://dx.doi.org/10.4172/2157-7587.1000157>

637 Hamed Y et al. (2014) Use of geochemical, isotopic, and age tracer data to develop models of
638 groundwater flow: A case study of Gafsa mining basin-Southern Tunisia Journal of
639 African Earth Sciences 100:418-436

640 Hastie TaRT (1986) Generalized additive models. Stat Sci 1:297-310
641 doi:[doi:10.1214/ss/1177013604](https://doi.org/10.1214/ss/1177013604).

642 Heinze G, Wallisch C, Dunkler D (2018) Variable selection—a review and recommendations for
643 the practicing statistician Biometrical Journal 60:431-449

644 Horton RE (1932) Drainage-basin characteristics Eos, transactions american geophysical union
645 13:350-361 doi:<https://doi.org/10.1029/TR013i001p00350>

646 Horton RE (1945) Erosional development of streams and their drainage basins; hydrophysical
647 approach to quantitative morphology Geological society of America bulletin 56:275-370
648 doi:[https://doi.org/10.1130/0016-7606\(1945\)56\[275:EDOSAT\]2.0.CO;2](https://doi.org/10.1130/0016-7606(1945)56[275:EDOSAT]2.0.CO;2)

649 Hosking JRM, Wallis JR (2005) Regional frequency analysis: an approach based on L-moments.
650 Cambridge University Press,

651 Howard AD (1990) Theoretical model of optimal drainage networks Water Resources Research
652 26:2107-2117 doi:<https://doi.org/10.1029/WR026i009p02107>

653 Jenson SK, Domingue JO (1988) Extracting topographic structure from digital elevation data for
654 geographic information system analysis Photogrammetric engineering and remote
655 sensing 54:1593-1600

656 Jung K, Marpu PR, Ouarda TB (2015) Improved classification of drainage networks using
657 junction angles and secondary tributary lengths Geomorphology 239:41-47
658 doi:<https://doi.org/10.1016/j.geomorph.2015.03.004>

659 Jung K, Marpu PR, Ouarda TB (2017) Impact of river network type on the time of concentration
660 Arabian Journal of Geosciences 10:546 doi:<https://doi.org/10.1007/s12517-017-3323-3>

661 Kaliraj S, Chandrasekar N, Magesh N (2015) Morphometric analysis of the River Thamirabarani
662 sub-basin in Kanyakumari District, South west coast of Tamil Nadu, India, using remote
663 sensing and GIS Environmental Earth Sciences 73:7375-7401
664 doi:<https://doi.org/10.1007/s12665-014-3914-1>

665 Kouider A, Gingras H, Ouarda T, Ristic-Rudolf Z, Bobée B (2002a) Analyse fréquentielle locale
666 et régionale et cartographie des crues au Québec Rep R-627-el

667 Kouider A, Ouarda T, Bobée B (2002b) Analyse fréquentielle locale des crues au Québec
668 doi:<http://espace.inrs.ca/365/1/T000342.pdf>

669 Latt ZZ, Wittenberg H, Urban B (2015) Clustering hydrological homogeneous regions and neural
670 network based index flood estimation for ungauged catchments: an example of the
671 Chindwin River in Myanmar Water resources management 29:913-928
672 doi:<https://doi.org/10.1007/s11269-014-0851-4>

673 Leclerc M, Ouarda TB (2007) Non-stationary regional flood frequency analysis at ungauged sites
674 Journal of hydrology 343:254-265 doi:<https://doi.org/10.1016/j.jhydrol.2007.06.021>

675 Máčka Z (2001) Determination of texture of topography from large scale contour maps.

676 Magesh N, Chandrasekar N, Soundranayagam JP (2011) Morphometric evaluation of Papanasam
677 and Manimuthar watersheds, parts of Western Ghats, Tirunelveli district, Tamil Nadu,

678 India: a GIS approach Environmental Earth Sciences 64:373-381
679 doi:<https://doi.org/10.1007/s12665-010-0860-4>

680 Marchi L, Dalla Fontana G (2005) GIS morphometric indicators for the analysis of sediment
681 dynamics in mountain basins Environmental Geology 48:218-228
682 doi:<https://doi.org/10.1007/s00254-005-1292-4>

683 Melton MA (1957) An analysis of the relations among elements of climate, surface properties,
684 and geomorphology. COLUMBIA UNIV NEW YORK,

685 Mesa L (2006) Morphometric analysis of a subtropical Andean basin (Tucuman, Argentina)
686 Environmental Geology 50:1235-1242 doi:<https://doi.org/10.1007/s00254-006-0297-y>

687 Miller VC (1953) quantitative geomorphic study of drainage basin characteristics in the Clinch
688 Mountain area, Virginia and Tennessee Technical report (Columbia University
689 Department of Geology); no 3

690 Msilini A, Masselot P, Ouarda TBMJ (2020) Regional Frequency Analysis at Ungauged Sites
691 with Multivariate Adaptive Regression Splines Journal of Hydrometeorology:1-1
692 doi:10.1175/jhm-d-19-0213.1

693 Muttiah RS, Srinivasan R, Allen PM (1997) PREDICTION OF TWO-YEAR PEAK STREAM-
694 DISCHARGES USING NEURAL NETWORKS JAWRA Journal of the American
695 Water Resources Association 33:625-630 doi:<https://doi.org/10.1111/j.1752-1688.1997.tb03537.x>

697 O'Callaghan JF, Mark DM (1984) The extraction of drainage networks from digital elevation data
698 Computer vision, graphics, and image processing 28:323-344
699 doi:[https://doi.org/10.1016/S0734-189X\(84\)80011-0](https://doi.org/10.1016/S0734-189X(84)80011-0)

700 Odry J, Arnaud P (2017) Comparison of Flood Frequency Analysis Methods for Ungauged
701 Catchments in France Geosciences 7:88 doi:<https://doi.org/10.3390/geosciences7030088>

702 Ouali D, Chebana F, Ouarda TBMJ (2016) Non-linear canonical correlation analysis in regional
703 frequency analysis Stochastic environmental research and risk assessment 30:449-462
704 doi:<https://doi.org/10.1007/s00477-015-1092-7>

705 Ouali D, Chebana F, Ouarda TBMJ (2017) Fully nonlinear statistical and machine-learning
706 approaches for hydrological frequency estimation at ungauged sites Journal of Advances
707 in Modeling Earth Systems 9:1292-1306 doi:<https://doi.org/10.1002/2016MS000830>

708 Ouarda TBMJ (2016) Regional flood frequency modeling chapter 77, in: VP Singh, (Ed) Chow's
709 Handbook of Applied Hydrology, 3rd Edition, Mc-Graw Hill, New York: pp. 77.71-77.78,
710 ISBN 978-970-907-183509-183501

711 Ouarda TBMJ, Charron C, Hundedcha Y, St-Hilaire A, Chebana F (2018) Introduction of the
712 GAM model for regional low-flow frequency analysis at ungauged basins and
713 comparison with commonly used approaches Environmental Modelling & Software
714 109:256-271 doi:<https://doi.org/10.1016/j.envsoft.2018.08.031>

715 Ouarda TBMJ, Girard C, Cavadias GS, Bobée B (2001) Regional flood frequency estimation with
716 canonical correlation analysis Journal of Hydrology 254:157-173
717 doi:[https://doi.org/10.1016/S0022-1694\(01\)00488-7](https://doi.org/10.1016/S0022-1694(01)00488-7)

718 Ouarda TBMJ, Haché M, Bruneau P, Bobée B (2000) Regional flood peak and volume estimation
719 in northern Canadian basin Journal of cold regions engineering 14:176-191
720 doi:[https://doi.org/10.1061/\(ASCE\)0887-381X\(2000\)14:4\(176\)](https://doi.org/10.1061/(ASCE)0887-381X(2000)14:4(176))

721 Pandey G, Nguyen V-T-V (1999) A comparative study of regression based methods in regional
722 flood frequency analysis Journal of Hydrology 225:92-101
723 doi:[https://doi.org/10.1016/S0022-1694\(99\)00135-3](https://doi.org/10.1016/S0022-1694(99)00135-3)

724 Pareta K, Pareta U (2011) Quantitative morphometric analysis of a watershed of Yamuna basin,
725 India using ASTER (DEM) data and GIS International journal of Geomatics and
726 Geosciences 2:248

727 Patton PC (1988) Drainage basin morphometry and floods Flood Geomorphology John Wiley &
728 Sons New York 1988 p 51-64 11 fig, 1 tab, 67 ref

729 Patton PC, Baker VR (1976) Morphometry and floods in small drainage basins subject to diverse
730 hydrogeomorphic controls Water Resources Research 12:941-952
731 doi:<https://doi.org/10.1029/WR012i005p00941>

732 Rahman A (2005) A quantile regression technique to estimate design floods for ungauged
733 catchments in south-east Australia Australian Journal of Water Resources 9:81-89
734 doi:<https://doi.org/10.1080/13241583.2005.11465266>

735 Rahman A, Charron C, Ouarda TBMJ, Chebana F (2018) Development of regional flood
736 frequency analysis techniques using generalized additive models for Australia Stochastic
737 Environmental Research and Risk Assessment 32:123-139
738 doi:<https://doi.org/10.1007/s00477-017-1384-1>

739 Rai PK, Mishra VN, Mohan K (2017) A study of morphometric evaluation of the Son basin, India
740 using geospatial approach Remote Sensing Applications: Society and Environment 7:9-
741 20 doi:<https://doi.org/10.1016/j.rsase.2017.05.001>

742 Ratnam KN, Srivastava Y, Rao VV, Amminedu E, Murthy K (2005) Check dam positioning by
743 prioritization of micro-watersheds using SYI model and morphometric analysis—remote
744 sensing and GIS perspective Journal of the Indian society of remote sensing 33:25
745 doi:<https://doi.org/10.1007/BF02989988>

746 Reddy GPO, Maji AK, Gajbhiye KS (2004) Drainage morphometry and its influence on landform
747 characteristics in a basaltic terrain, Central India—a remote sensing and GIS approach
748 International Journal of Applied Earth Observation and Geoinformation 6:1-16
749 doi:<https://doi.org/10.1016/j.jag.2004.06.003>

750 Requena AI, Ouarda TBMJ, Chebana F (2018) Low-flow frequency analysis at ungauged sites
751 based on regionally estimated streamflows Journal of Hydrology
752 doi:<https://doi.org/10.1016/j.jhydrol.2018.06.016>

753 Ridolfi E, Rianna M, Trani G, Alfonso L, Di Baldassarre G, Napolitano F, Russo F (2016) A new
754 methodology to define homogeneous regions through an entropy based clustering method
755 Advances in Water Resources 96:237-250
756 doi:<https://doi.org/10.1016/j.advwatres.2016.07.007>

757 Schumm SA (1956) Evolution of drainage systems and slopes in badlands at Perth Amboy, New
758 Jersey Geological society of America bulletin 67:597-646
759 doi:[https://doi.org/10.1130/0016-7606\(1956\)67\[597:EODSAS\]2.0.CO;2](https://doi.org/10.1130/0016-7606(1956)67[597:EODSAS]2.0.CO;2)

760 Seckin N (2011) Modeling flood discharge at ungauged sites across Turkey using neuro-fuzzy
761 and neural networks Journal of hydroinformatics 13:842-849
762 doi:<https://doi.org/10.2166/hydro.2010.046>

763 Seidou O, Ouarda T, Barbet M, Bruneau P, Bobee B (2006) A parametric Bayesian combination
764 of local and regional information in flood frequency analysis *Water resources research* 42
765 doi: <https://doi.org/10.1029/2005WR004397>

766 Shaban A, Khawlie M, Abdallah C, Awad M (2005) Hydrological and watershed characteristics
767 of the El-Kabir River, North Lebanon Lakes & Reservoirs: *Research & Management*
768 10:93-101 doi:<https://doi.org/10.1111/j.1440-1770.2005.00262.x>

769 Shu C, Ouarda T (2008) Regional flood frequency analysis at ungauged sites using the adaptive
770 neuro-fuzzy inference system *Journal of Hydrology* 349:31-43
771 doi:<https://doi.org/10.1016/j.jhydrol.2007.10.050>

772 Shu C, Ouarda TBMJ (2007) Flood frequency analysis at ungauged sites using artificial neural
773 networks in canonical correlation analysis physiographic space *Water Resources*
774 *Research* 43 doi:doi:10.1029/2006WR005142

775 Sivasena Reddy A, Janga Reddy M (2013) Identification of homogenous regions in rain-fed
776 watershed using Kohonen neural networks *ISH Journal of Hydraulic Engineering* 19:55-
777 66 doi:<https://doi.org/10.1080/09715010.2013.763408>

778 Smith A, Sampson C, Bates P (2015) Regional flood frequency analysis at the global scale *Water*
779 *Resources Research* 51:539-553 doi: <https://doi.org/10.1002/2014WR015814>

780 Sreedevi P, Srekanth P, Khan H, Ahmed S (2013) Drainage morphometry and its influence on
781 hydrology in an semi arid region: using SRTM data and GIS *Environmental earth*
782 *sciences* 70:839-848 doi:<https://doi.org/10.1007/s12665-012-2172-3>

783 Sreedevi P, Subrahmanyam K, Ahmed S (2005) The significance of morphometric analysis for
784 obtaining groundwater potential zones in a structurally controlled terrain *Environmental*
785 *Geology* 47:412-420 doi:<https://doi.org/10.1007/s00254-004-1166-1>

786 Stall JB, Fok Y-S Discharge as related to stream system morphology. In: *International*
787 *Association of Scientific Hydrology Symposium on River Morphology*, Publication,
788 1967. pp 224-235

789 Strahler (1953) Revisions of Horton's quantitative factors in erosional terrain *Trans Am Geophys*
790 *Union* 34:345

791 Strahler (1957) Quantitative analysis of watershed geomorphology *Eos, Transactions American*
792 *Geophysical Union* 38:913-920 doi:<https://doi.org/10.1029/TR038i006p00913>

793 Strahler (1964) Part II. Quantitative geomorphology of drainage basins and channel networks
794 *Handbook of Applied Hydrology*: McGraw-Hill, New York:4-39

795 Strahler A (1952) Hypsometric (area-altitude) analysis of erosional topography *Geological*
796 *Society of America Bulletin* 63:1117-1142 doi:[https://doi.org/10.1130/0016-7606\(1952\)63\[1117:HAAOET\]2.0.CO;2](https://doi.org/10.1130/0016-7606(1952)63[1117:HAAOET]2.0.CO;2)

797

798 Taofik OK, Innocent B, Christopher N, Jidauna GG, James AS (2017) A Comparative Analysis
799 of Drainage Morphometry on Hydrologic Characteristics of Kereke and Ukoghor Basins
800 on Flood Vulnerability in Makurdi Town, Nigeria *Hydrology* 5:32 doi:doi:
801 10.11648/j.hyd.20170503.11

802 Tarboton DG, Bras RL, Rodriguez-Iturbe I (1991) On the extraction of channel networks from
803 digital elevation data *Hydrological processes* 5:81-100

804 Trambly Y, Ouarda TBMJ, St-Hilaire A, Poulin J (2010) Regional estimation of extreme
805 suspended sediment concentrations using watershed characteristics *Journal of Hydrology*
806 380:305-317 doi:<https://doi.org/10.1016/j.jhydrol.2009.11.006>

807 Tsakiris G, Nalbantis I, Cavadias G (2011) Regionalization of low flows based on canonical
808 correlation analysis Advances in water resources 34:865-872
809 doi:<https://doi.org/10.1016/j.advwatres.2011.04.007>

810 Verstappen H (1983) Applied Geomorphology. Elsevier, Amsterdam-Oxford-New York,
811 Vijith H, Satheesh R (2006) GIS based morphometric analysis of two major upland sub-
812 watersheds of Meenachil river in Kerala Journal of the Indian Society of Remote Sensing
813 34:181-185 doi:<https://doi.org/10.1007/BF02991823>

814 Wan Jaafar W, Liu J, Han D (2011) Input variable selection for median flood regionalization
815 Water Resources Research 47 doi:10.1029/2011WR010436,

816 Wazneh H, Chebana F, Ouarda TB (2016) Identification of hydrological neighborhoods for
817 regional flood frequency analysis using statistical depth function Advances in water
818 resources 94:251-263 doi:<https://doi.org/10.1016/j.advwatres.2016.05.013>

819 Wood (2006) Generalized additive models: an introduction with R. CRC press,
820 Youssef AM, Pradhan B, Hassan AM (2011) Flash flood risk estimation along the St. Katherine
821 road, southern Sinai, Egypt using GIS based morphometry and satellite imagery
822 Environmental Earth Sciences 62:611-623 doi:[https://doi.org/10.1007/s12665-010-0551-](https://doi.org/10.1007/s12665-010-0551-1)
823 [1](https://doi.org/10.1007/s12665-010-0551-1)

824

825

826

827

828

829

830

831

832

833

834

835

836

837

838 **List of tables**

839 Table 1 Predictor variables used in a number of previous regionalization studies.36
840 Table 2 Morphometric variables definitions.....37
841 Table 3 Correlation between hydrological and physiographical variables.....38
842 Table 4 Variables selection results for QS₁₀ case (with different methods).38
843 Table 5 Descriptive statistics of new physiographical variables.....39
844 Table 6 Explanatory variables selected for the various regression models.39
845 Table 7 Jackknife Validation Results.....40

846

847 **List of Figures**

848 Fig.1 Different combinations and considered models.....41
849 Fig.2 Backward elimination process.42
850 Fig. 3 Geographical location of the studied stations in Quebec, Canada.43
851 Fig. 4 Relative errors associated to the local quantile QS₁₀₀ calculated with ROI/GAM/STA and
852 ROI/GAM/EXTD.....44
853 Fig. 5 Relative errors associated to the local quantile QS₁₀₀ calculated with CCA/GAM/STA and
854 CCA/GAM/EXTD.44
855 Fig. 6 Relative errors using ROI/GAM/STA and ROI/GAM/EXTD as a function of QS₁₀₀.....44
856 Fig. 7 Specific regional quantile versus local estimates using ROI/GAM/STA and
857 ROI/GAM/EXTD approaches for QS₁₀₀.....45
858 Fig. 8 Specific regional quantile versus local estimates using CCA/GAM/STA and
859 CCA/GAM/EXTD approaches for QS₁₀₀.45
860 Fig. 9 Smooth functions of QS₁₀₀ for the predictor variables included in the regional models
861 ALL/GAM/STA, CCA/GAM/STA and ROI/GAM/STA. The dotted lines represent the 95%
862 confidence intervals. The vertical axes denote the spline of each explanatory variable.46
863 Fig. 10 Smooth functions of QS₁₀₀ for the predictor variables included in the regional models
864 ALL/GAM/EXTD, CCA/GAM/EXTD and ROI/GAM/EXTD. The dotted lines represent the 95%
865 confidence intervals. The vertical axes denote the spline of each explanatory variable.47

866

867

868

869

870

871

872

Table 1 Predictor variables used in a number of previous regionalization studies.

References	Country	Predictor variables adopted
(Muttiyah et al. 1997)	USA	Catchment areas, mean annual rainfall, and mean basin elevation.
(Rahman 2005)	Australia	Catchment area, design rainfall intensity, mean annual rainfall, mean annual rain days, mean annual Class A pan evaporation, mainstream slope, lemniscate shape, river bed elevation at the gauging station, maximum elevation difference in the basin, stream density, forest cover, and fraction quaternary sediment area.
(Dawson et al. 2006)	United Kingdom	Catchment area, base flow index, standard percentage runoff, index of flood attenuation attributable to reservoirs and lakes, standard period (1961-1990) average annual rainfall, median annual maximum 1-day rainfall, median annual maximum 2-day rainfall, median annual maximum 1-h rainfall, mean Soil Moisture Deficit for 1941-1970, proportion of time when Soil Moisture Deficit <6 mm during 1961-1990, longest drainage path, mean distance between each node (on a regular 50 m grid) and catchment outlet, mean altitude of catchment above sea level, mean of all inter-nodal slopes in the catchment, invariability of slope directions, extent of urban and suburban land cover in 1990.
(Leclerc and Ouarda 2007)	Canada	Catchment area, gauging station latitude, gauging station longitude, mean total winter/spring precipitation, mean winter/spring maximum air temperature.
(Leclerc and Ouarda 2007)	USA	Catchment area, mean annual rainfall, runoff measured, mainstream slope, main-channel length, forest cover, and storage measured as the percent of the catchment area.
(Griffis and Stedinger 2007)	Canada	Catchment area, mean annual rainfall, mean basin slope, the fraction of the basin area covered with lakes and annual mean degree days below 0 °C.
(Shu and Ouarda 2008) (Alobaidi et al. 2015) (Durocher et al. 2015) (Ouali et al. 2016) (Wazneh et al. 2016)	Mexico	Drainage area, mean annual precipitation, final altitude of the mainstream and slope of the main stream.
(Castiglioni et al. 2009)	Italy	Drainage area, main channel length, the percentage of permeable area, maximum, minimum and mean elevations, average elevation relative to the minimum elevations, concentration time, mean annual temperature and mean annual temperature precipitation.
(Wan Jaafar et al. 2011)	England	Catchment area, longest flow path, basin length, basin perimeter, form factor, average slope, maximum relief, relief ratio, drainage density, stream frequency, bifurcation ratio, length of overland flow, land use (agriculture), land use (forest), land use (residential), land use (water and wetland), soil type (coarse), soil type (medium), soil type (medium fine), soil type (fine), soil type (peat soil) and rainfall.
(Seekin 2011)	Turkey	Drainage area, elevation, latitude, longitude and return period.
(Flavell 2012)	Australia	Catchment area, mean annual rainfall, mainstream slope, main-channel length, and 12 and 24 h statistical rainfall totals.
(Haddad and Rahman 2012)	Australia	Catchment area, design rainfall intensity, mean annual rainfall, mean annual evapotranspiration, stream density, mainstream slope, stream length, and forest cover.
(Beck et al. 2013)	3394 basins around the world.	Humidity index, mean annual precipitation, precipitation seasonality, mean annual potential evaporation, potential evaporation seasonality, seasonal correlation between water supply and demand, mean annual air temperature, mean snow water equivalent depth, mean elevation, mean surface slope, fraction of open water, fraction of forest, mean Normalized Difference Vegetation Index (NDVI), mean permeability of consolidated and unconsolidated geologic units below the soil, mean gravel content, mean sand content, mean silt content, mean clay content.
(Aziz et al. 2014)	Australia	Catchment area, design rainfall intensity values $I(tc)$ with where $ARI = 2, 5, 10, 20, 50$ and 100 years return period ($tc =$ time of concentration), mean annual rainfall, mean annual areal evapotranspiration, and mainstream slope.
(Castellarin 2014)	Italy	Drainage area, mainstream length, maximum, mean, and minimum elevations, mean annual temperature, net annual precipitation, annual potential evapotranspiration, coefficients of L variation of the net annual precipitation, annual potential evapotranspiration, percentage of previous area, the long-term mean daily stream flow standardized by the catchment area, and the daily stream flow associated with a duration of 355 days standardized by catchment.
(Latt et al. 2015)	Myanmar	Catchment area, mean basin elevation, basin slope, basin length, shape factor, soil conservation curve number, time of concentration, mean annual rainfall.
(Smith et al. 2015)	Several basins across the world.	Catchment area, average annual rainfall and the upstream catchment slope.
(Ridolfi et al. 2016)	Italy	Catchment area, the previous area, the maximum and mean altitudes, the gauge elevation, the mean slope, the length and the slope of the longest drainage path (LDP), annual mean precipitation, and the coordinates of each site.
(Odry and Arnaud 2017)	France	Aridity index, annual mean evapotranspiration, annual mean solid precipitation, annual mean liquid precipitation, annual mean temperature, annual mean soil moisture, mean soil moisture prior to a rainy event (>20 mm), mean duration of rainfall events, mean number of rainfall events per season, mean intensity of rainfall events, river network density, mean elevation, mean slope, capacity of the production reservoir of a lumped rainfall-runoff model, presence of sand bedding, presence of rock bedding, low infiltration capacity class, medium infiltration capacity class, high infiltration capacity class, forest cover, arable cover, grassland cover, catchment area, catchment eastening (X) and catchment northing (Y).
(Hailegeorgis and Alfredsen 2017)	Mid-Norway	Catchment area,
(Requena et al. 2018)	Canada	Catchment area, fraction of the catchment controlled by lakes, fraction of the catchment occupied by forest, annual mean degree-days below 0 °C, summer mean liquid precipitation, curve number and average number of days with mean temperature greater than 27 °C.
(Rahman et al. 2018)	Australia	Catchment area, catchment shape factor, main stream slope, stream density, percentage of catchment covered by forest, rainfall intensity (6 h duration and 2 year return period), mean annual rainfall and mean annual potential evapotranspiration.

874

875

876

Table 2 Morphometric variables definitions.

Morphometric variables	Formula / Relationship	Reference
Stream order (u) (*)	Hierarchical order	(Horton 1945; Strahler 1957)
Stream Length (Lu) (*)	Length of stream	(Horton 1945)
Texture ratio (RT)	$RT = \frac{N_1}{P}$, where N_1 = the number of first order streams and P = perimeter (km).	(Schumm 1956)
Circularity Ratio (RC) (*)	$RC = 4 \pi \left(\frac{A}{P^2}\right)$, where A = area of the basin (km^2), P = perimeter of the basin (km) and $\pi = 3.1415$.	(Miller 1953)
Stream length ratio (RL)	$RL = \frac{MLu}{Lu-1}$, where MLu = the average stream length of a given order u (km) and $MLu-1$ = the average stream length of the next lower order (km).	(Horton 1945)
Mean stream length ratio (MRL)	MRL = Average of the stream length ratio of all orders	(Horton 1945)
Bifurcation ratio (RB)	$RB = \frac{Nu}{Nu+1}$, Nu = the number of stream segments of order u , $Nu + 1$ = the number of stream segments of the next higher order.	(Horton 1945)
Mean bifurcation ratio (MRB) (*)	MRB = Average of bifurcation ratios of all orders	(Strahler 1957)
Weighted mean bifurcation ratio (WMRB)	$WMRB = \frac{\sum RB_{(u)}(Nu+Nu+1)}{\sum N}$, where $RB_{(u)}$ = the bifurcation ratio between each successive pair of orders, Nu = the total number of stream segments of order u and $\sum N$ = the total number of streams involved in the ratio.	(Schumm 1956; Strahler 1953)
RHO coefficient (ρ)	$\rho = \frac{RL}{RB}$	(Horton 1945)
RHO $_{WMRB}$ coefficient (ρ_{WMRB})	$\rho_{WMRB} = \frac{RL}{WMRB}$	(Horton 1945; Schumm 1956; Strahler 1953)
Drainage density (DD) (*)	$DD = \frac{L}{A}$, where L = total stream length of all orders (km), A = area of the basin (km^2).	(Horton 1932; Horton 1945)
Stream frequency (FS) (*)	$FS = \frac{N}{A}$, where N = total number of streams of all orders and A = area of the basin (km^2).	(Horton 1932; Horton 1945)
Infiltration number (IF)	$IF = DD \times FS$	(Faniran 1968)
Basin Relief (BH)	The highest elevation of the basin - Lowest elevation of the basin (km)	(Schumm 1956; Strahler 1957)
Ruggedness number (RN)	$RN = BH \times DD$, where BH = Basin relief and DD = Drainage density.	(Melton 1957)
PN1	Percentage of first-order streams	(Patton and Baker 1976)
PL1	Percentage of first-order stream lengths	(Blyth and Rodda 1973)

878

879 (*) Variables previously used in regional hydrological frequency analysis studies, but not
880 used with the Quebec data base.

881

882

883

884

Table 3 Correlation between hydrological and physiographical variables.

	QS ₁₀	QS ₅₀	QS ₁₀₀
AREA	-0.46	-0.45	-0.44
MBS	0.47	0.46	0.46
PLAKE	-0.67	-0.65	-0.63
MATP	0.68	0.64	0.62
DDBZ	-0.60	-0.60	-0.59
LONGC	0.47	0.45	0.44
RT	-0.53	-0.52	-0.51
RC	0.68	0.66	0.65

885

886

Table 4 Variables selection results for QS₁₀ case (with different methods).

Models Variables	STA								EXTD							
	LLRM				GAM				LLRM				GAM			
	Fd	Bd	Sw	Sh	Fd	Bd	Sw	Sh	Fd	Bd	Sw	Sh	Fd	Bd	Sw	Sh
AREA	*	*	*	*	*	*	*	*	*	*	*	*				
MCL				*				*				*		*		*
MCS				*	*							*				
MBS	*	*	*	*	*		*	*					*			
PFOR	*	*	*	*	*		*	*	*	*	*	*	*	*	*	*
PLAKE	*	*	*	*	*	*	*	*	*	*	*	*	*	*	*	*
MATP	*				*			*	*				*	*		
MALP	*	*	*	*	*	*		*	*	*	*	*	*		*	
MASP					*				*	*	*					*
MALPS				*			*					*				*
DDBZ	*	*	*	*	*	*		*	*	*	*	*		*		
LATC														*		
LONGC	*	*	*	*	*	*	*	*	*	*	*	*			*	*
RT									*		*			*	*	*
RC												*	*	*	*	*
MRL									*	*	*	*	*	*	*	*
MRB									*	*	*		*			
WMRB									*	*	*	*	*		*	*
ρ_{WMRB}																
DD									*	*	*	*	*	*	*	*
FS										*				*		
IF										*			*	*		
RN									*	*	*	*	*	*		*
PN1												*		*		*
PL1										*			*			

887 Fd is Forward ; Bd is backward; Sw is stepwise selection and Sh is shrinkage approach selection.

888

889

Table 5 Descriptive statistics of new physiographical variables.

Variable	Min	Mean	Max	STD.dev
DD (Km ⁻¹)	2.41	2.96	4.73	0.34
FS (Km ⁻²)	7.34	9.74	11.86	0.97
IF (Km ⁻³)	17.69	29.26	67.09	6.56
RT (Km ⁻¹)	8.09	32.11	131.84	21.41
MRB	1.67	2.40	17.27	2.08
WMRB	1.95	2.08	4.14	0.24
MRL	0.85	0.97	1.11	0.05
ρ_{WMRB}	0.23	0.47	0.55	0.04
RN	0.20	1.89	7.48	1.03
RC	0.06	0.18	0.46	0.08
PN1 (%)	50.12	50.41	52.50	0.30
PL1 (%)	44.09	52.89	66.36	4.10

890

891

Table 6 Explanatory variables selected for the various regression models.

Regional models	Quantile	Selected predictor variables
ALL/LLRM/STA,CCA/LLRM/STA,ROI/LLRM/STA	QS ₁₀	AREA, MBS, PFOR, PLAKE, MALP, DDBZ, LONGC
	QS ₅₀	AREA, MBS, PFOR, PLAKE, MALP, DDBZ, LONGC
	QS ₁₀₀	AREA, MBS, PFOR, PLAKE, MATP, MALP, LONGC
ALL/LLRM/EXTD,CCA/LLRM/EXTD,ROI/LLRM/EXTD	QS ₁₀	AREA, PFOR, PLAKE, MALP, DD , MRL , LONGC
	QS ₅₀	AREA, PFOR, PLAKE, MALP, DD , MRL , LONGC
	QS ₁₀₀	AREA, PFOR, PLAKE, MALP, DD , MRL , LONGC
ALL/GAM/STA,CCA/GAM/STA,ROI/GAM/STA	QS ₁₀	AREA, MBS, PLAKE, MALP, MASP, DDBZ, LONGC
	QS ₅₀	AREA, MCL, MBS, PLAKE, MALP, DDBZ, LONGC
	QS ₁₀₀	AREA, MCL, MBS, PLAKE, MALP, DDBZ, LONGC
ALL/GAM/EXTD,CCA/GAM/EXTD,ROI/GAM/EXTD	QS ₁₀	MCL, PLAKE, MATP, DDBZ, DD , RN , LATC
	QS ₅₀	MCL, PLAKE, MALP, DDBZ, DD , MRL , LONGC
	QS ₁₀₀	MCL, PLAKE, MALP, DDBZ, DD , MRL , LONGC

892 Variables dealing with drainage network characteristics are in bold character.

Table 7 Jackknife Validation Results.

Quantile		ALL/LLRM		ALL/GAM		CCA/LLRM		CCA/GAM		ROI/LLRM		ROI/GAM	
		STA	EXTD	STA	EXTD	STA	EXTD	STA	EXTD	STA	EXTD	STA	EXTD
NASH	QS ₁₀	0,669	0.641	0.774	0.802	0.799	0.808	0.797	0.837	0.807	0.804	0.829	0.865
	QS ₅₀	0,620	0.587	0.745	0.754	0.731	0.743	0.762	0.775	0.754	0.750	0.796	0.816
	QS ₁₀₀	0.609	0.556	0.715	0.725	0.680	0.706	0.723	0.742	0.703	0.720	0.762	0.791
RMSE [(m ³ /s)km ²]	QS ₁₀	0,073	0.076	0.060	0.056	0.057	0.056	0.057	0.051	0.056	0.056	0.053	0.047
	QS ₅₀	0,109	0.113	0.089	0.087	0.092	0.089	0.086	0.080	0.087	0.088	0.080	0.076
	QS ₁₀₀	0.125	0.133	0.107	0.105	0.113	0.108	0.105	0.101	0.109	0.106	0.097	0.091
RRMSE (%)	QS ₁₀	43.528	41.202	40.937	34.970	37.412	32.760	37.163	30.619	34.418	31.584	34.690	27.974
	QS ₅₀	48.518	44.891	49.420	36.659	42.232	36.520	43.333	35.086	39.251	34.034	39.365	27.818
	QS ₁₀₀	50.682	46.918	51.832	38.630	46.259	38.426	45.678	37.416	41.497	35.214	41.661	29.235
BIAIS [(m ³ /s)km ²]	QS ₁₀	0.004	0.003	0.005	0.005	0.007	0.008	0.006	0.007	0.008	0.009	0.003	0.004
	QS ₅₀	0.008	0.006	0.008	0.008	0.015	0.017	0.015	0.015	0.013	0.015	0.006	0.009
	QS ₁₀₀	0.011	0.007	0.011	0.011	0.020	0.022	0.020	0.020	0.015	0.019	0.009	0.012
RBIAIS (%)	QS ₁₀	-6,161	-5.936	-5.461	-4.179	-6.023	-4.587	-5.555	-3.871	-3.040	-0.932	-4.177	-2.836
	QS ₅₀	-7,338	-6.892	-7.047	-4.954	-6.293	-4.238	-5.632	-3.513	-4.358	-1.175	-5.487	-2.892
	QS ₁₀₀	-7.782	-7.431	-7.663	-5.472	-6.623	-4.305	-5.780	-3.714	-4.881	-1.381	-5.816	-3.172

894 Best results are in bold character.

895

896

909
910
911
912
913
914
915
916
917
918
919
920
921
922

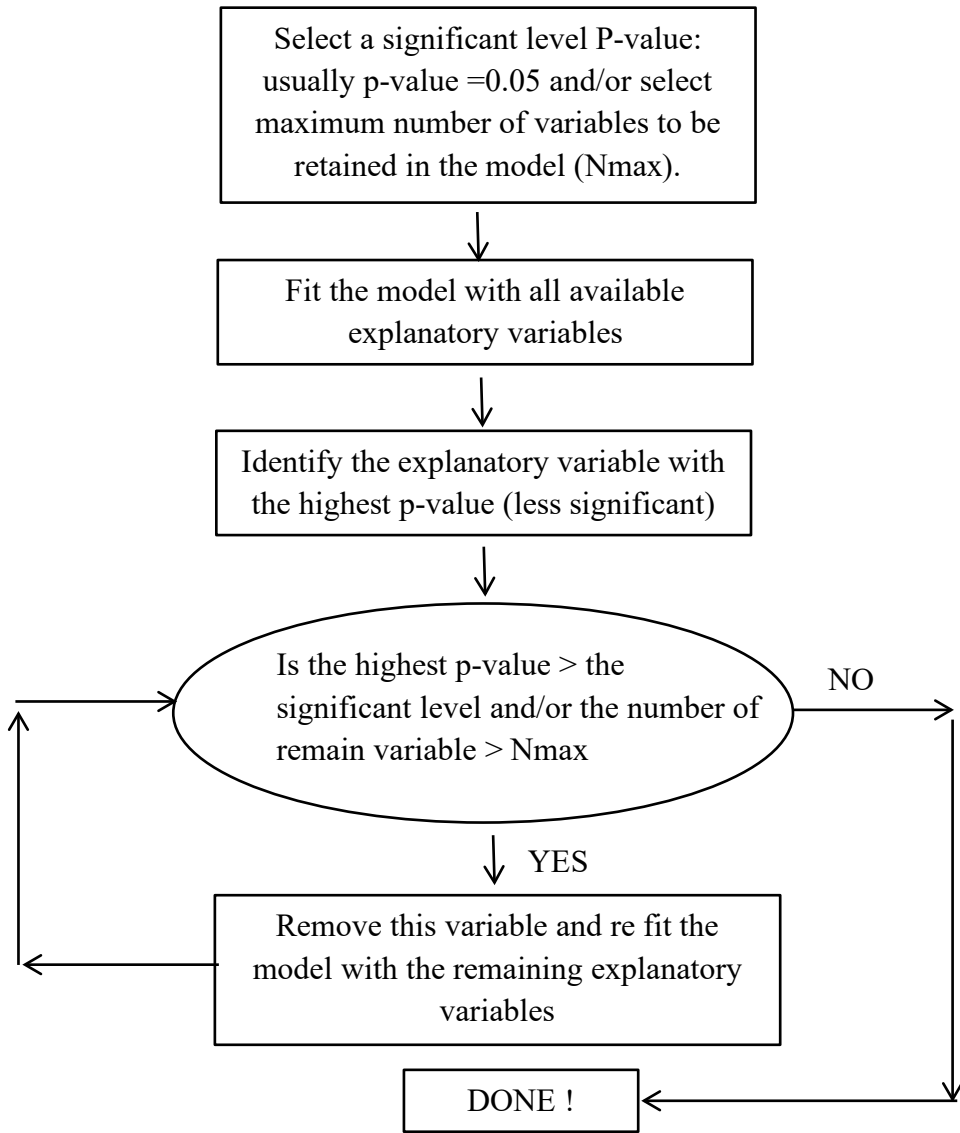
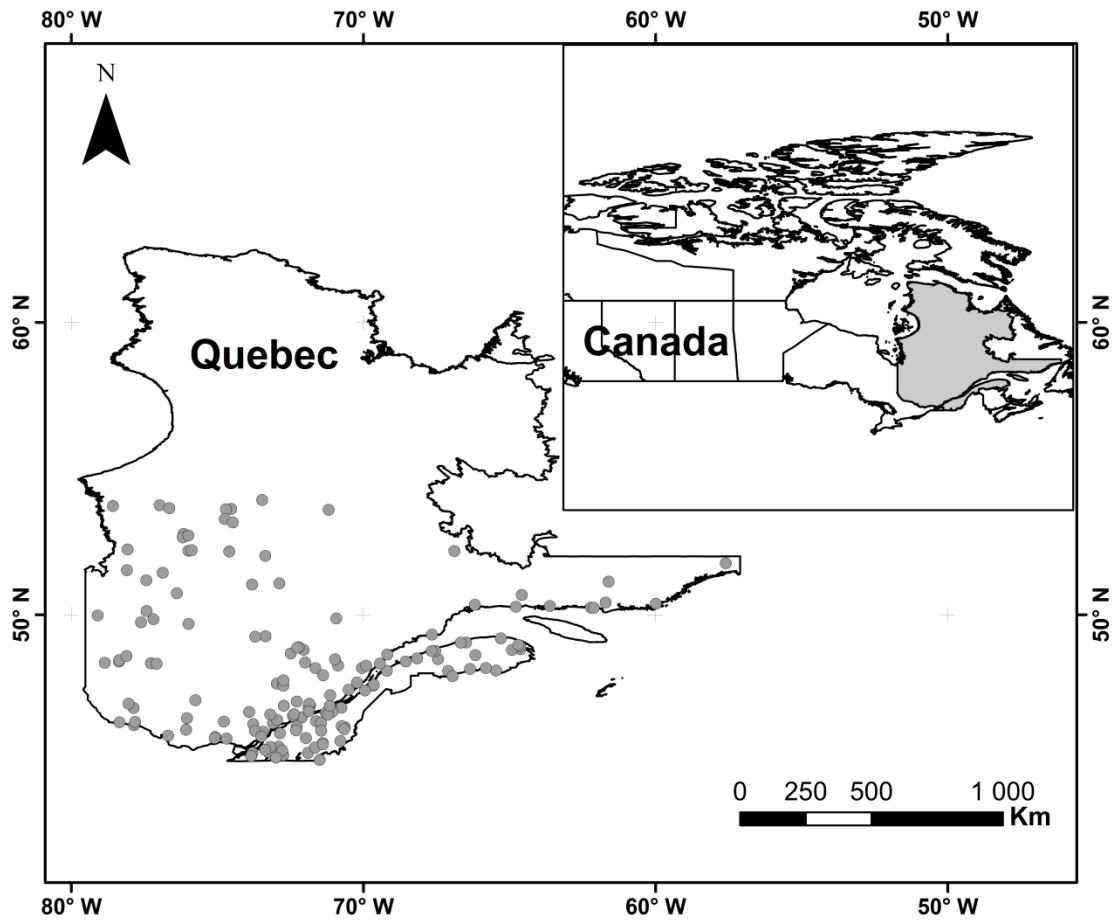
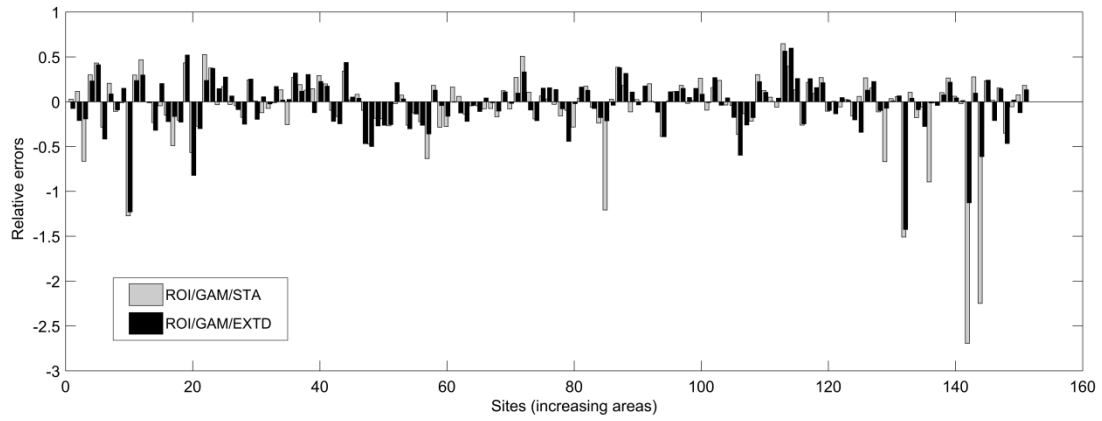


Fig.2 Backward elimination process.



923
924
925
926
927
928
929
930

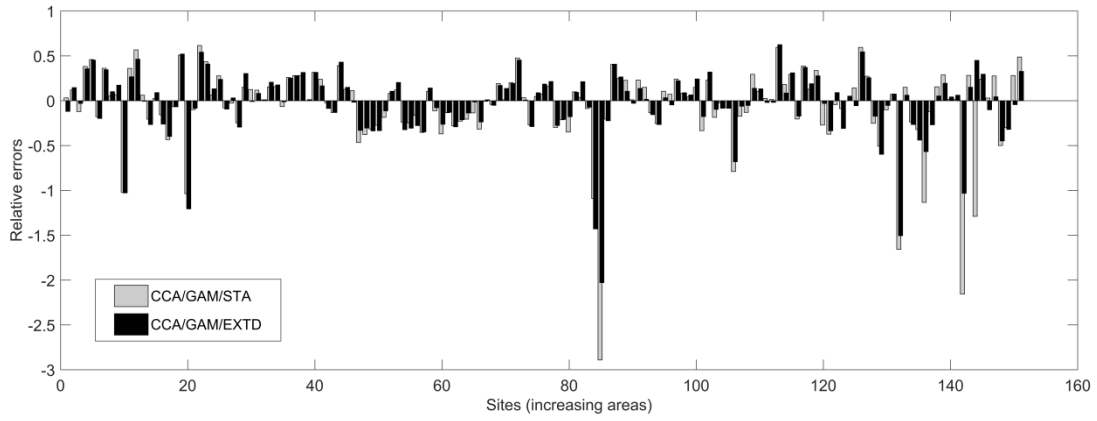


931

932

933

ROI/GAM/EXTD.

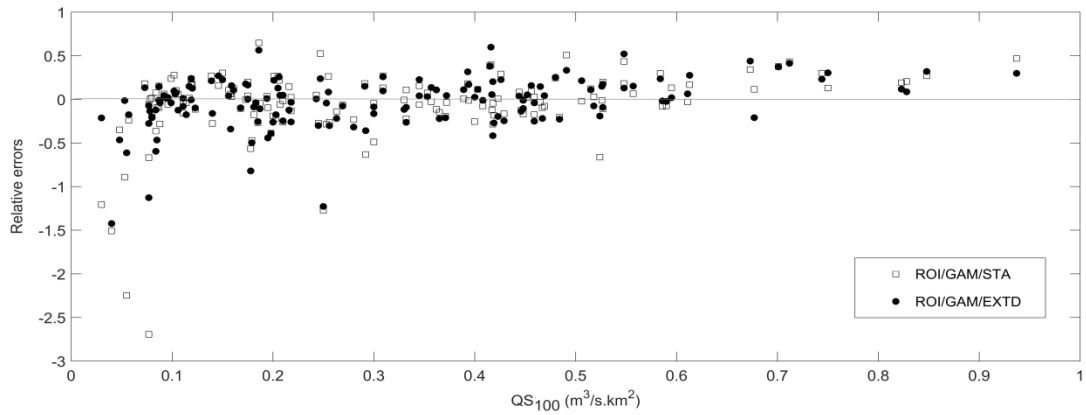


934

935

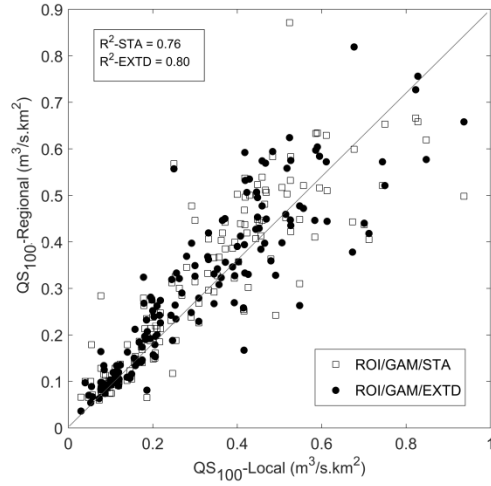
936

CCA/GAM/EXTD.



937

938



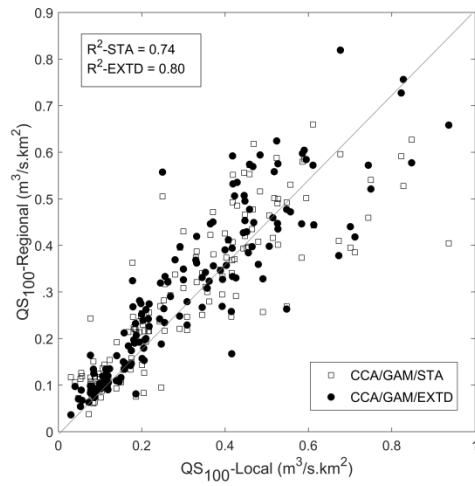
939

940

941

approaches for QS₁₀₀.

942

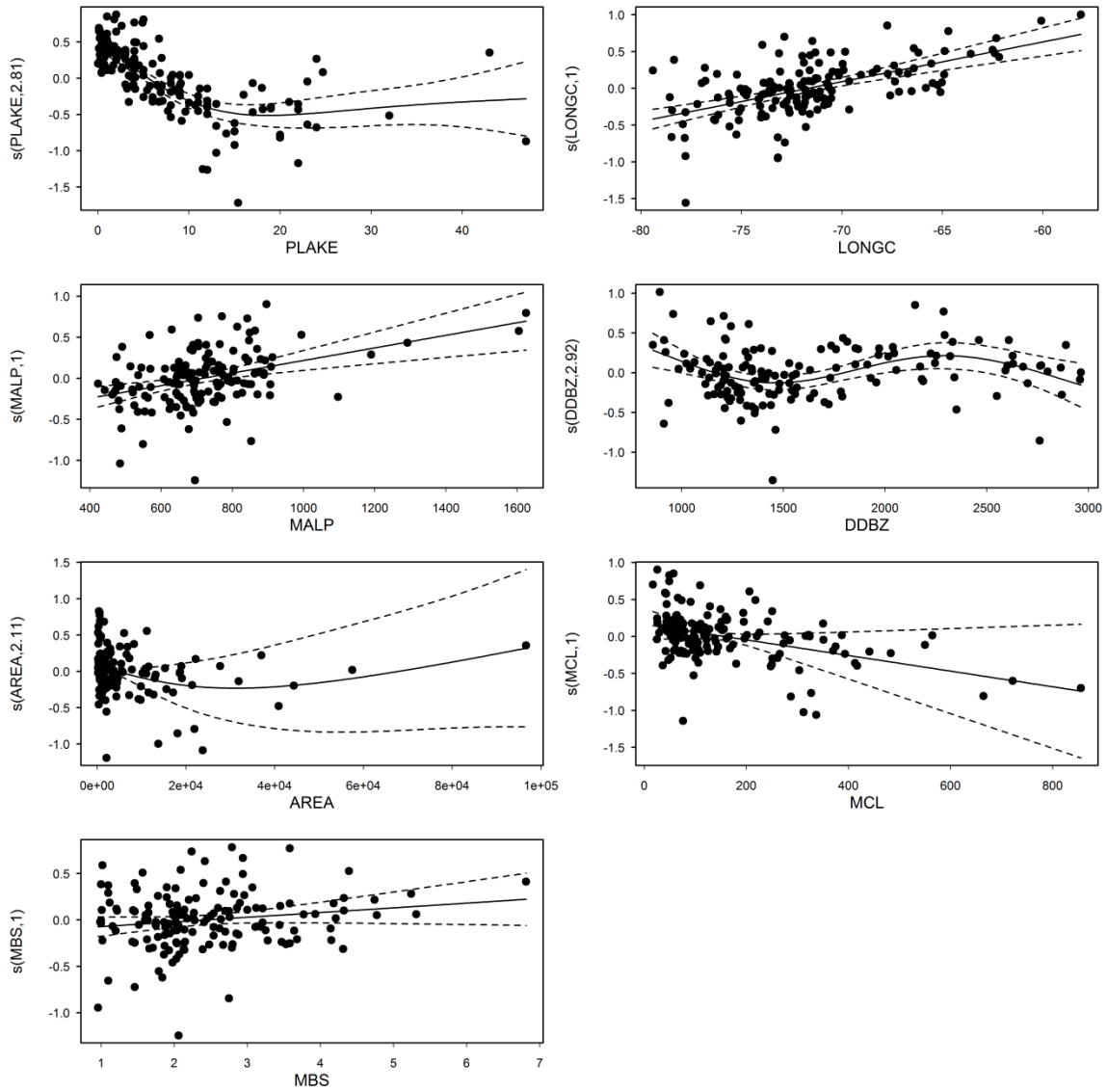


943

944

945

approaches for QS₁₀₀.



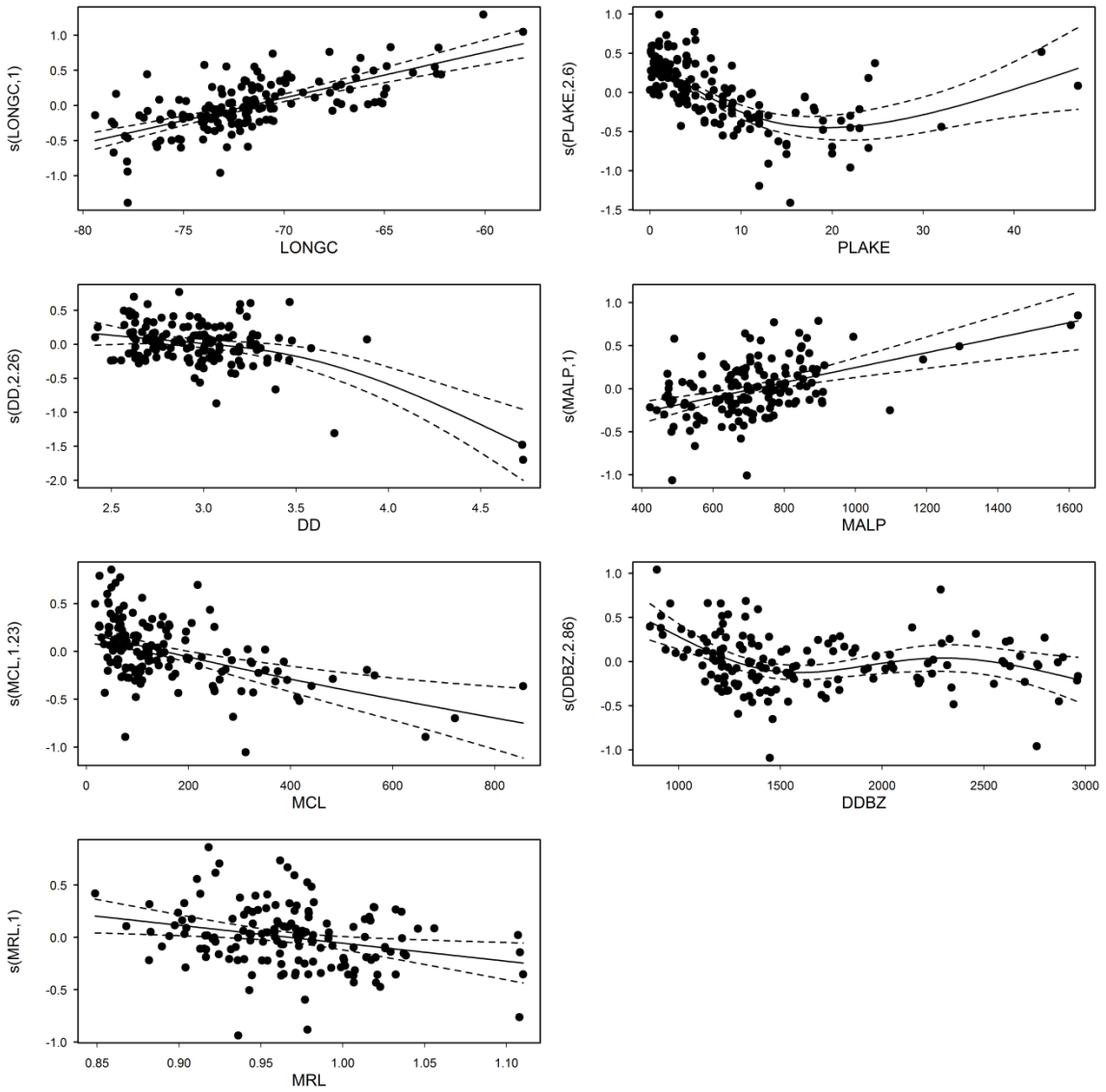
946

947

948 ALL/GAM/STA, CCA/GAM/STA and ROI/GAM/STA. The dotted lines represent the 95% confidence

949

intervals. The vertical axes denote the spline of each explanatory variable.



950

951

952 ALL/GAM/EXTD, CCA/GAM/EXTD and ROI/GAM/EXTD. The dotted lines represent the 95%
 953 confidence intervals. The vertical axes denote the spline of each explanatory variable.

954

955

956

957

958